scientific reports

Check for updates

OPEN

Diverse antifungal potency of terbinafine as a therapeutic agent against *Exophiala dermatitidis* in vitro

Tomofumi Nakamura[1,2,5]✉, Tatsuya Yoshinouchi[1,5], Mayu Okumura[2], Toshiro Yokoyama[3], Daisuke Mori[1], Hirotomo Nakata[2], Jun-ichirou Yasunaga[2] & Yasuhito Tanaka[1,4]

Exophiala dermatitidis **(*E. dermatitidis*), which causes skin or respiratory disease, is occasionally fatal in immunocompromised patients. Here, we report the unique antifungal potency of terbinafine (TRB), which targets squalene epoxidase, against *E. dermatitidis* (SQLE^{ED}) using various in vitro approaches. The versatile antifungal activities, including fungicidal activity, biofilm formation inhibition, biofilm eradication activity, and the combination effect of TRB, posaconazole (PSC), and amphotericin B (AmB) with great antifungal potency against *E. dermatitidis* were evaluated using crystal violet and cell viability assay. TRB formed an H-bond through Y102 in SQLE^{ED} in the binding model. *E. dermatitidis* hyphae elongated and attached to a cell scaffold, forming a membrane-like biofilm. TRB and PSC showed more potent antibiofilm activities than AmB, and exhibited post-antifungal effects without incubation against *E. dermatitidis* conidia, reducing growth at lower concentrations. In contrast, AmB exhibited strong dose- and time-dependent killing and biofilm-eradication activities. The combination of TRB and PSC was more effective than that of TRB and AmB or PSC and AmB. Although the tissue migration of TRB must be considered, these data suggest that TRB and PSC may be useful agents and a potent combination in severely immunocompromised patients with refractory and systemic *E. dermatitidis* infection.**

Keywords *Exophiala dermatitidis*, Terbinafine, Posaconazole, Amphotericin B, Biofilm

It is estimated that 1.7 billion people worldwide suffer from fungal infections[1]. Invasive fungal infections in patients undergoing organ transplantation, chemotherapy for cancer, human immunodeficiency virus (HIV) infection, or autoimmune diseases cause approximately 1.7 million deaths per year[2].

Exophiala dermatitidis (*E. dermatitidis*) is a black fungus, a member of the Herpotrichiellaceae, that can be isolated from wet living environments such as dishwashers, humidifiers, and bathtubs[3], and is commonly reported as a pathogen of black fungal infections isolated from the skin and subcutaneous tissue in dermatological treatment[4]. Respiratory tract infections caused by *E. dermatitidis* are relatively rare, with reports of underlying diseases such as bronchiectasis and cystic fibrosis[5,6]. Moreover, black fungal infections caused by *E. dermatitidis* isolated from the skin, eye, liver, central nervous system, and central venous catheters have been reported as opportunistic fatal infections in immunocompromised patients[7]. *E. dermatitidis* has a slower growth rate than the other fungi. Small black colonies of *E. dermatitidis* observed on Sabouraud dextrose agar (SDA) after 3 days were barely detectable. Matrix-assisted laser desorption ionization-time of flight mass spectrometry (MALDI-TOF MS) is a powerful tool for the early identification of pathogenic fungal species, including late-growing fungi such as *E. dermatitidis*, in addition to morphological and genetic analysis of the specimen[8]. We previously reported *E. dermatitidis* pneumonia in immunocompromised patients with anorexia nervosa[9]. In clinical practice, *E. dermatitidis* is treated with azoles such as voriconazole or itraconazole for several months[10,11]. In this study, we analyzed characteristics of *E. dermatitidis* and evaluated the antifungal, antibiofilm, post-antifungal effects (PAFE), killing (fungicidal) activity, and combinations of several clinically used oral and intravenous

[1]Department of Laboratory Medicine, Kumamoto University Hospital, Kumamoto, Japan. [2]Department of Hematology, Rheumatology, and Infectious Diseases, Faculty of Life Sciences, Kumamoto University, Kumamoto, Japan. [3]Department of Medical Technology, Faculty of Health Science, Kumamoto Health Science University, Kumamoto, Japan. [4]Department of Gastroenterology and Hepatology, Faculty of Life Sciences, Kumamoto University, Kumamoto, Japan. [5]These authors contributed equally: Tomofumi Nakamura and Tatsuya Yoshinouchi. ✉email: tomona@kumamoto-u.ac.jp

antifungal agents such as terbinafine (TRB)[12], azoles (fluconazole [FLC], miconazole [MCZ], voriconazole [VRC], itraconazole [ITC], posaconazole [PSC], isavuconazole [ISC])[13], micafungin (MCF), caspofungin (CAS), and amphotericin B (AmB)[14] against *E. dermatitidis*. The aim of this study is to elucidate the potential of TRB in vitro against *E. dermatitidis*.

Results

Profile of clinically isolated *E. dermatitidis*

We observed giant black colonies of *E. dermatitidis* 1 isolated from a clinical patient[9] under aerobic incubation at room temperature on SDA and performed morphological observations using an optical microscope and scanning electron microscope (SEM) (Fig. 1). The center of the giant colonies formed a black gelatinous mass and the surface and edges changed to olive brown (Fig. 1A). Microscopy revealed many yeast-like oval conidia in the center (Fig. 1B) and septate hyphae and hyphae in the outer part of the black colony (Fig. 1B). The internal transcribed spacer 1 (ITS1) and D1/D2 regions of the large subunit of the 28S ribosomal RNA gene were compared using the Basic Local Alignment Search Tool (BLAST). The identification rate of the D1/D2 region was dominated by *Exophiala* species, and that of *E. dermatitidis* was 96.9%, and the ITS region was 100% identical to *E. dermatitidis* (Fig. S1A). Based on genetic analysis of the ITS region, we identified the giant black fungus as *E. dermatitidis* genotype A (Fig. S1B), which is most commonly reported in Japan[15].

Next, we analyzed the growth of *E. dermatitidis* 1 at 25, 30, 37, and 40 ℃. The growth gradually increased from 36 to 108 h and was more efficient at 30 and 37 ℃ than at 25 and 40 ℃ in MOPS-RPMI (Fig. 1C) and sabouraud medium (Fig. S1C). In addition, the diameter of the black colonies of *E. dermatitidis* 1 on SDA incubated for a week was 8.8, 8.0, 7.0, and 6.3 mm at 30, 37, 25, and 40 ℃, respectively, in line with the growth results at these temperatures (Fig. 1D). These results suggest that the growth of *E. dermatitidis* was affected by incubation temperature; in particular, incubation at 40 ℃ prevented the growth. The benefit of thermotherapy in cutaneous or subcutaneous infections has been previously reported[16].

Structural modeling of *E. dermatitidis* squalene epoxidase

Target proteins of various antifungal drugs in clinical use are shown in Fig. 2A. TRB target squalene epoxidase (SQLE), also known as squalene monooxygenase, which catalyzes the conversion of squalene to (S)-2,3-epoxy squalene, is a key enzyme in ergosterol biosynthesis in fungal membranes[17,18]. Azoles can also exert anti-fungal activity by inhibiting a different target enzyme, lanosterol 14α-demethylase in the same pathway as shown in Fig. 2A.[19].

To investigate the structural antifungal efficacy of TRB against *E. dermatitidis*, we identified the $SQLE^{ED}$ derived from three *E. dermatitidis* (Table S1) with the same amino acid (AA) sequences. The AA sequences of SQLEs from humans, *E. dermatitidis*, and *Trichophyton rubrum* (*T. rubrum*) were compared using Clustal omega (multiple sequence alignment tool), as shown in Table S1. Moreover, the structural modeling of $SQLE^{ED}$ was produced by SWISS-MODEL based on the crystallography of human SQLE ($SQLE^{Hum}$) (PDB:6C6N) as previously reported[18] and the full-length $SQLE^{Hum}$ model shown in Fig. 2B and S2A. Next, we performed a docking simulation of TRB to $SQLE^{ED}$ (Fig. 2B) based on the crystal structure of Cmpd-4 bound to $SQLE^{Hum}$ (PDB:6C6N) using SeeSAR (see Methods). The top 20 structures of the TRB bound to $SQLE^{ED}$ are shown in Fig. S2C. The TRB-binding structures of $SQLE^{Hum}$ and $SQLE^{ED}$ formed hydrogen bonds with the side chains of Tyr 122 and 102, respectively (Fig. S2). Important AA residues (L393, F397, F415, and H440) of SQLE ($SQLE^{TR}$) that bind to TRB have been reported in the resistance profiles of clinical isolates of *T. rubrum* (Fig. S2D)[20]. TRB is surrounded by L410, F414, F432, and H459 of $SQLE^{ED}$, which correspond to L393, F397, F415, and H440 of $SQLE^{TR}$ in the binding as shown in Fig. 2C. These results indicate that TRB can effectively interact with $SQLE^{ED}$, resulting in a potent antifungal activity against *E. dermatitidis* (Table 1 and Table S2).

Antifungal activity of clinically used drugs against *E. dermatitidis*

Various orally and intravenously administered antifungal drugs are available for clinical use. In this study, we evaluated the antifungal effects of ten drugs (FLC, MCZ, VRC, ITC, PSC, ISC, TRB, AmB, CAS, and MCF) (Fig. 3A and Fig. S3) against clinically isolated *E. dermatitidis* 1 (Table 1) based on the CLSI M38-Ed3. Additionally, the susceptibilities of the other two *E. dermatitidis* strains (E.D.2, clinically isolated, and E.D.3, ATCC28869) to TRB, PSC, and AmB were evaluated (Table S2). The minimum inhibitory concentration (MIC), 50% inhibition of growth (MIC_{50}), and 90% inhibition of growth (MIC_{90}) were determined using $OD_{530,}$ or OD_{440} after WST-1 reagent staining to evaluate the viability of *E. dermatitidis* (WST-1 assay)[21]. As previously reported[22,23], the MICs of FLC, MCF, and CAS against *E. dermatitidis* exceeded 16 mg/L. PSC, VRC, AmB, TRB, and ITC showed potent inhibitory activity from 0.031 to 0.25 mg/L against *E. dermatitidis* at MIC by visual observation or at MIC_{50} and MIC_{90} by measurement of OD_{530} or OD_{440} (WST-1) (Table 1). MCZ at 0.25 to 0.5 mg/L inhibited the growth similarly to ISC. The MIC of all drugs was found to be very close to the MIC_{90} value obtained from WST-1 assay. *E. dermatitidis* exhibited different growth rates at different temperatures (Fig. 1C and Fig. S1C). To examine the effect of the incubation temperature on antifungal activity, we determined MIC_{50} and MIC_{90} of drugs by measuring *E. dermatitidis* growth at $OD_{530.}$ (Table S3). The findings indicated that incubation temperature did not significantly affect the antifungal activity of these drugs.

Inhibition and eradication of *E. dermatitidis*-induced biofilm

Bacterial and fungal biofilms form in infected organs, particularly on medical devices such as intravascular catheters, artificial heart valves, and artificial joints, causing intractable chronic infections, which is resistant to antibiotics and antifungals[24]. It has been reported that *E. dermatitidis* can produce biofilm formation[25].

The chemical structures of TRB, PSC, and AmB are shown in Fig. 3A. When *E. dermatitidis* 1 was treated with TRB, PSC, and AmB at 0.125 mg/L, different morphologies of *E. dermatitidis* conidia were observed. The

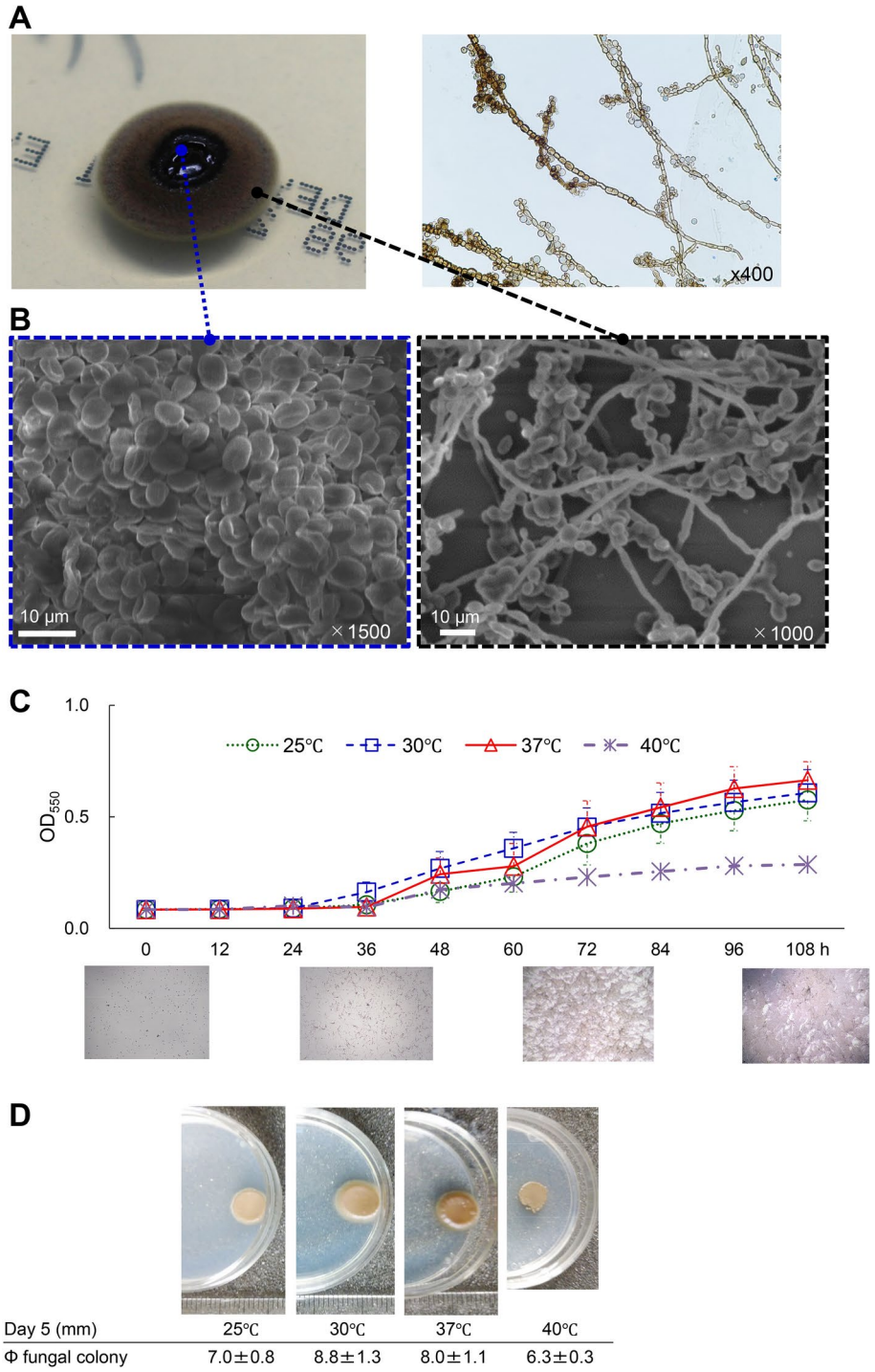

Fig. 1. Characteristics of *E. dermatitidis*. (**A**) A single colony of *E. dermatitidis* 1 was grown on an SDA plate for 14 days. The lactophenol cotton blue-stained specimen image was observed using the slide culture method. (**B**) Morphological image of the central and marginal areas of *E. dermatitidis* colony by SEM. The scale bar and magnification at each image are shown (**C**) the growth rate was determined every 12 h up to 108 ho at 25, 30, 37, and 40℃, and microscopic images at 37℃ were taken at 0, 36, 72, and 108 h in MOPS-RPMI culture medium until 108 h or (**D**) colonies on the SDA plate for 120 h at 25, 30, 37, and 40℃, respectively.

E. dermatitidis conidia and hyphae were dense in TRB and AmB, while the *E. dermatitidis* conidia were diffuse in PSC (Fig. 3B). In addition, *E. dermatitidis* 1 was incubated with or without A549 cells in a glass-bottomed slide chamber plate. The *E. dermatitidis* without A549 cells floated in the buffer, whereas the *E. dermatitidis* with A549 cells firmly attached to the bottom of the slide (Fig. S3). Next, we investigated the morphology of the *E. dermatitidis* with or without A549 cells by optical microscopy (Fig. S3A) and SEM. (Fig. 3). The coadunate

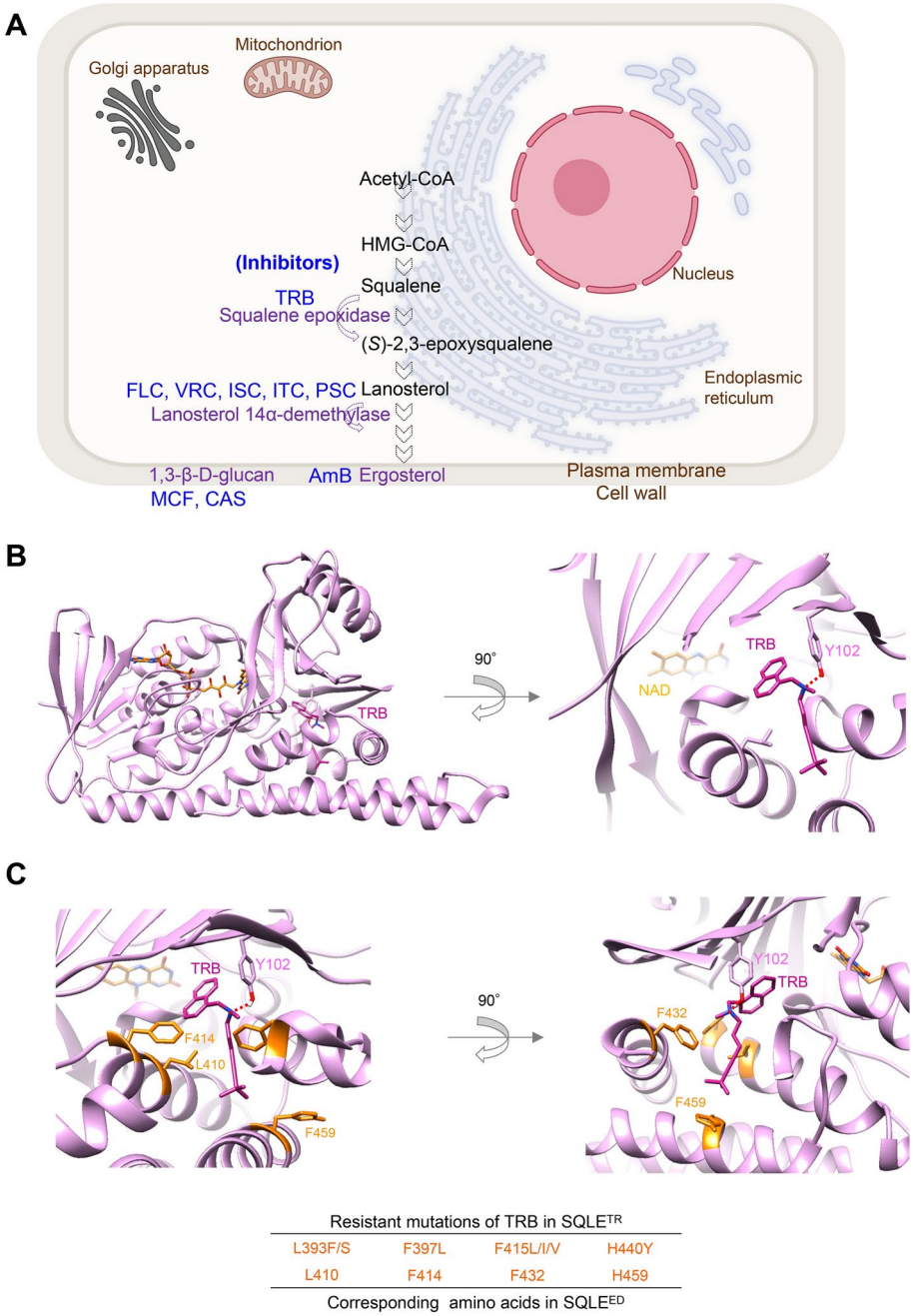

Fig. 2. Targets of antifungal drugs and SQLE structures. (**A**) Schematic illustration of antifungal target proteins in fungal cells. (**B**) The best binding model of TRB to the SQLE structure of *E. dermatitidis* with nicotinamide adenine dinucleotide (NAD). TRB interacts with Y102 through an H-bond in $SQLE^{ED}$. (**C**) The location of putative TRB-resistant amino acid residues (L410, F414, F432, and H459) in the $SQLE^{ED}$ structure corresponding to clinically TRB-resistant mutations (L393F/S, F397L, F415L/I/V, and H440Y) in the $SQLE^{TR}$.

filamentous biofilm-like morphology of the *E. dermatitidis* was sparsely observed without A549 cells as observed by SEM (Fig. S3B). On the other hand, the *E. dermatitidis* hyphae extended cohesively below and above the cells, and the oval conidia were diffusely attached to the cells for 24 h of incubation (Fig. 3C). Moreover, membrane biofilm-like morphology including the cells appeared where the *E. dermatitidis* was highly enriched for 48 h of incubation (Fig. 3D and Fig. S3B). Treatment with TRB, PSC, and AmB at 0.25 mg/L inhibited hypha growth and showed pseudohyphae of the *E. dermatitidis* (Fig. 3E). There were no clear differences in the *E. dermatitidis* morphology between these drug treatments in this condition.

Next, we examined the inhibitory and eradication abilities of TRB, PSC, and AmB against *E. dermatitidis*-induced biofilms using a CV assay (Fig. 4 and Fig. S4). Interestingly, TRB and PSC showed more potent inhibitory activity against the biofilm formation by *E. dermatitidis* 1 (Fig. 4B), and the antibiofilm activity of these drugs was similar to their antifungal activity (Fig. S4). In contrast, AmB sufficiently and TRB slightly at

	OD_{530}		OD_{440} (WST-1)			
Drugs	**MIC_{50}**	**MIC_{90}**	**MIC_{50}**	**MIC_{90}**	**MIC**	**MEC**
TRB	0.13	0.25	0.13	0.25	0.25	–
FLC	4	8	8	16	16	–
MCZ	0.5	0.5	0.25	0.5	0.5	–
VRC	0.063	0.13	0.13	0.13	0.13	–
ISC	0.13	1	0.25	1	1	–
ITC	0.25	0.25	0.13	0.25	0.25	–
PSC	0.063	0.13	0.031	0.13	0.13	–
AmB	0.063	0.13	0.063	0.13	0.13	–
MCF	8	32	16	32	–	8
CAS	8	32	16	32	–	8

Table 1. The susceptibility of *E. dermatitidis* 1 to the drugs. Minimum inhibitory concentration, MIC (mg/L) is defined as the lowest concentration of drugs that can be visually observed to inhibit the growth of clinical isolate *E. dermatitidis* 1. MIC_{50} and MIC_{90} values are determined as the lowest drug concentrations capable of inhibiting the *E. dermatitidis* 1 growth by 50% or 90%, respectively, as measured at OD_{530} nm. MIC_{50} and MIC_{90} of WST-1 are determined as the lowest drug concentrations capable of inhibiting 50% or 90%, respectively, of the *E. dermatitidis* 1 viability, as measured at OD_{440} nm after staining with WST-1. Minimum effective concentration (MEC) is defined as the lowest concentration of drugs that have any effect on *E. dermatitidis* 1.

high concentration eradicated the *E. dermatitidis*-induced biofilm compared to PSC (Fig. 4C). These results indicate that TRB and PSC can inhibit biofilm formation at lower concentrations than AmB. However, a higher concentration of AmB can moderately eradicate the biofilm-formed *E. dermatitidis* 1, suggesting that TRB and PSC may be useful in the early treatment of acute *E. dermatitidis* infection and that AmB may be effective in the late or prolonged treatment of chronic biofilm-formed *E. dermatitidis*. 1.

Fungicidal activity and combination effects of antifungal drugs against *E. dermatitidis*

The ability to kill invasive fungi is important in immunocompromised conditions[26]. We examined various antifungal effects of TRB, PSC, and AmB on *E. dermatitidis* using WST-1 reagent to examine living *E. dermatitidis*.

First, we evaluated the residual potency of the drugs, PAFE[27], on *E. dermatitidis* 1. Notably, the growth of *E. dermatitidis conidia* could be inhibited by TRB, PSC, and AmB without incubation, which washed the drugs immediately after administration (see Materials and Methods). (Fig. 5A, B). TRB and PSC at low concentrations (from 0.5 to 2.0 mg/L) decreased the growth of the *E. dermatitidis* compared to AmB, indicating that TRB and PSC can rapidly interact with and maintain the target proteins. TRB has been reported to have fungicidal activity against dermatophytes including *T. rubrum*[28]. In contrast, TRB did not show a time- and dose-dependent ability to kill the *E. dermatitidis* conidia, even at the highest concentration of 32 mg/L (Fig. 5C) in line with *Exophiala spinifera*[27]. The viability of *E. dermatitidis* 1 after treatment with TRB decreased compared to positive controls (no drug) up to 12 h, but incubation for 3, 6, and 12 h at all tested TRB concentrations increased compared to no incubation (0-h), indicating a reactive response of the *E. dermatitidis* to TRB. These data suggest that TRB has a fungistatic effect on *E. dermatitidis* conidia (Fig. 5C), whereas PSC and AmB killed *E. dermatitidis* conidia in a dose- and time-dependent manner (Fig. 5D, E).

In vitro and in vivo combination therapies are effective in treating refractory and chronic infections[29]. TRB and other antifungal combinations have been reported against *E. dermatitidis* and other fungi.[22,29,30] We investigated the combinations of antifungal drugs such as TRB and azoles (PSC, VRC, and ITC), TRB and AmB, and TRB and CAS against *E. dermatitidis* 1 (Fig. 6 and Fig. S5). A previous study[22] showed a synergistic effect against *E. dermatitidis* when CAS was combined with azoles (VRC and ITC) in vitro. The fractional inhibitory concentration index (FICI) was calculated from the MIC, MIC_{50}, and MIC_{90} values of WST-1 assay. The values for CAS and PSC were < 0.5, indicating a synergistic effect (Fig. S5). The value for the combination of TRB and AmB was between 1.0 and 2.0, and that for PSC and AmB between 1.0 and 2.2, resulting in no interaction effects (Fig. 6). However, when a combination of TRB with other azoles was examined, the FICI of TRB and PSC showed better efficacy between 0.31 and 0.75, TRB and ISC between 0.63 and 1.0, TRB and ITC at 0.5, and TRB and VRC between 0.63 and 1.0, indicating synergistic or no interaction effects (Fig. 6 and Fig. S5). These results suggest that the combination of TRB with azoles that inhibit different target proteins in the same pathway[29], (Fig. 2A) particularly ITC and PSC, was more favorable than AmB against *E. dermatitidis*.

Taken together, TRB may be a therapeutic agent with potent antifungal, anti-biofilm, PAFE, and fungistatic inhibition against *E. dermatitidis*, further when combined with azoles including PSC (Table 2).

Discussion

Systemic and invasive *E. dermatitidis* infections such as pneumonia and sepsis require a relatively long treatment period[10,11], and have been reported to result in death[8]. Therefore, potent antifungal activity including PAFE and fungicidal activity as well as tissue migration of antifungals to the site of infection are essential factors

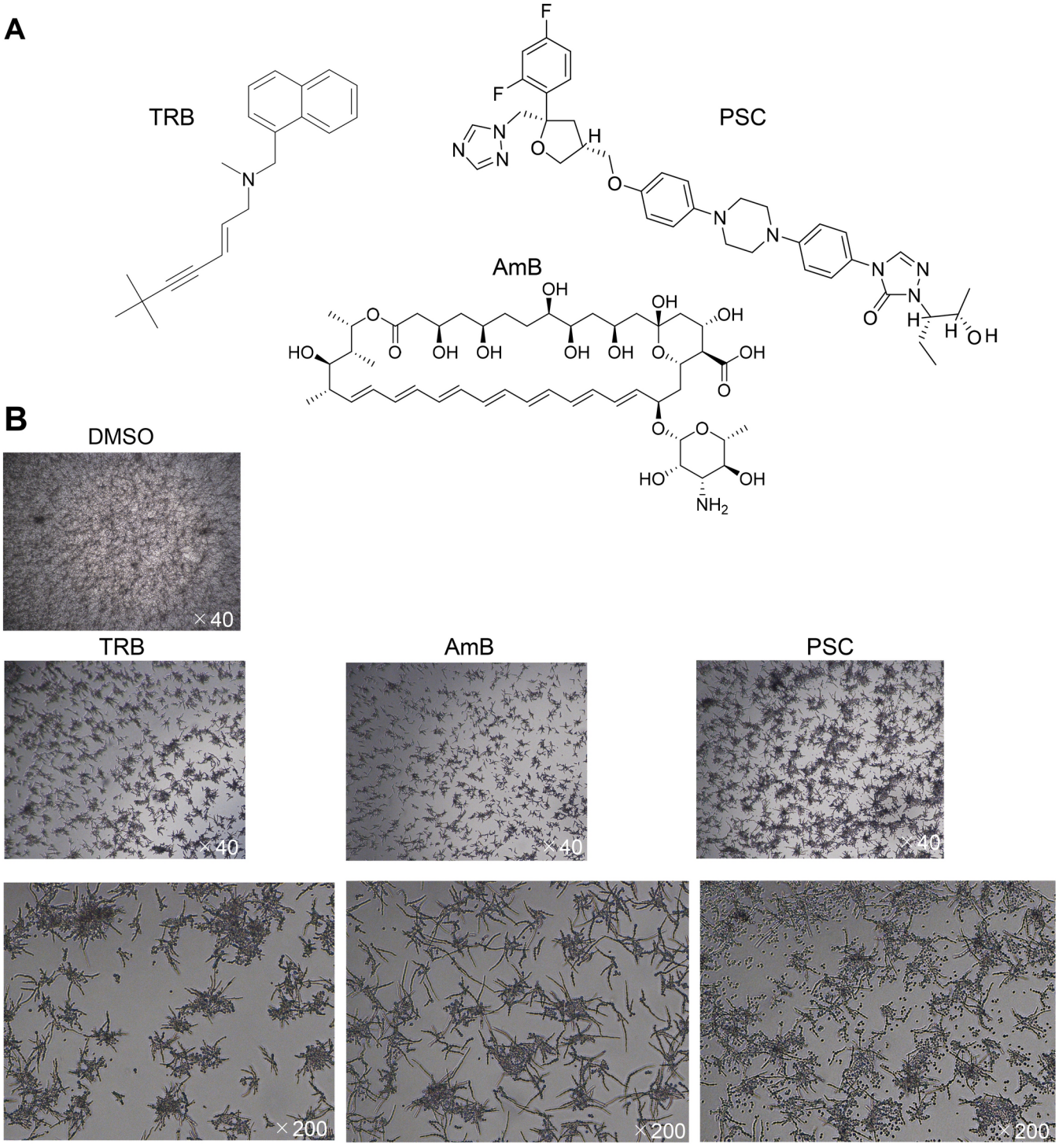

Fig. 3. Morphology of *E. dermatitidis* and drug efficacy of TRB, PSC, and AmB. (**A**) Chemical structures of TRB, PSC, and AmB. (**B**) Morphology of *E. dermatitidis* 1 in the presence of TRB, AmB, and PSC at 0.125 mg/L after incubation at 35℃ for 48 h in MOPS-RPMI buffer. (**C**) The *E. dermatitidis* hyphae were elongated and attached to the 549 cells indicated by yellow arrows after incubation at 35℃ for 24 h by SEM. (**D**) Gray-membrane biofilm containing A549 cells circled at the dotted yellow line formed on enriched *E. dermatitidis* 1 after incubation at 35℃ for 48 h. (**E**) *E. dermatitidis* 1 incubated on the A549 cells at 35℃ for 24 h in the presence of TRB, AmB, and PSC at 0.25 mg/L. The scale bar and magnification at each image are shown in white.

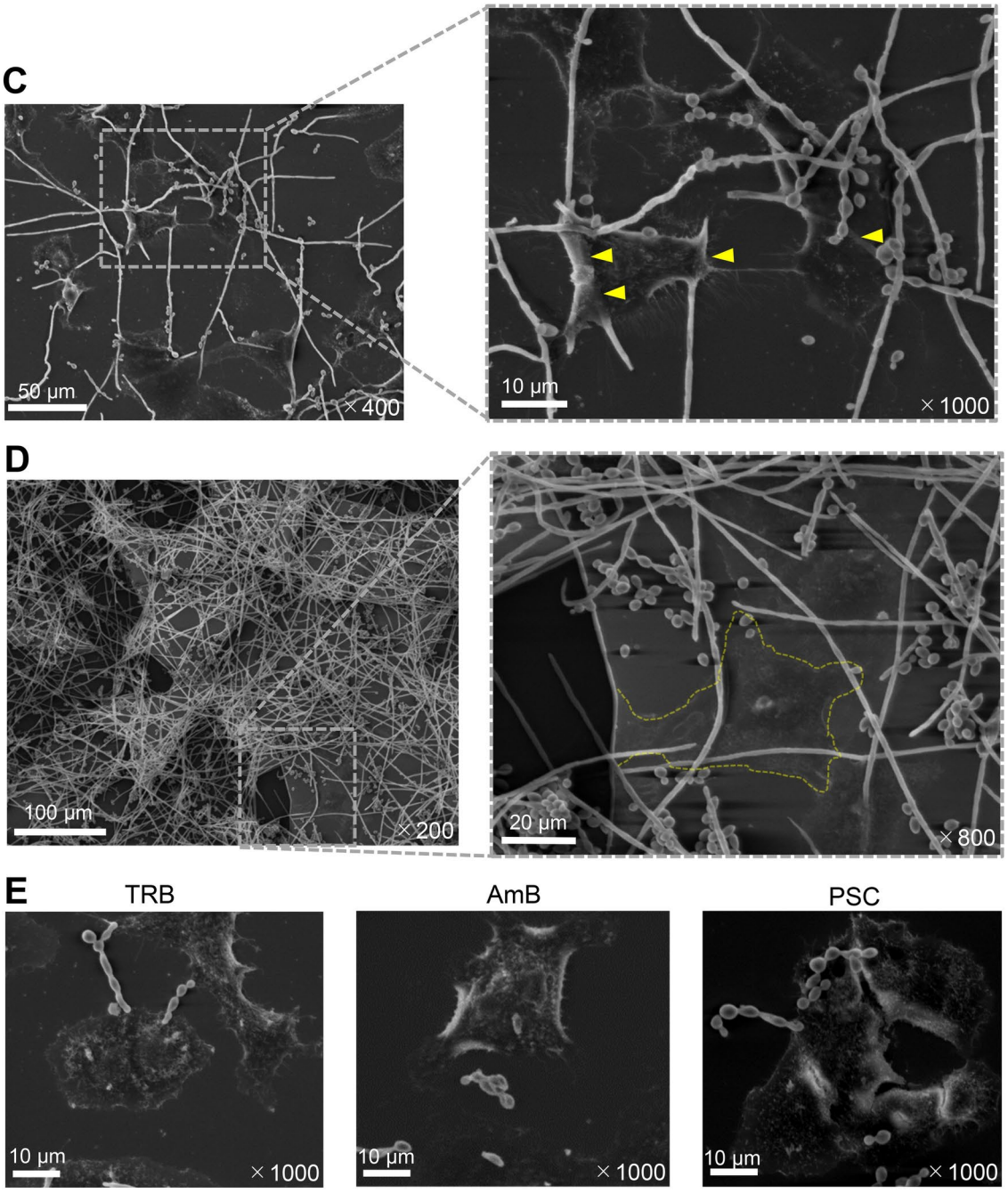

Figure 3. (continued)

for antifungal treatment when treating immunocompromised patients. TRB has been available as a useful therapeutic agent for trichophytosis in clinical practice[20,31].

In this study, TRB showed potent antifungal activity against *E. dermatitidis* in various in vitro assays, similar to that of PSC. In addition, TRB and PSC showed a stronger anti-biofilm effect of *E. dermatitidis* than AmB. Treatment of *E. dermatitidis* conidia with TRB of 0 h incubation decreased the growth of *E. dermatitidis* as a PAFE (Fig. 4A); however, TRB did not show a time- and dose-dependent killing ability against *E. dermatitidis* conidia even at the highest concentration, 32 mg/L (Fig. 5C). TRB can suppress the growth of *E. dermatitidis* from the conidia, but cannot kill them, suggesting that TRB has fungistatic effects against *E. dermatitidis* conidia as previously report of same genus, *E. spinifera*[27].

On the other hand, the biofilm eradication ability of TRB shown in Fig. 4C is slightly higher than that of PSC. Moreover, when we performed the growth inhibition assay to determine MIC, $MIC_{50,}$ and MIC_{90} at OD_{530} and OD_{440} (WST-1 assay). TRB was found to inhibit the growth of *E. dermatitidis* at low concentrations similar to PSC with fungicidal activity against *E. dermatitidis* (Fig. S4).

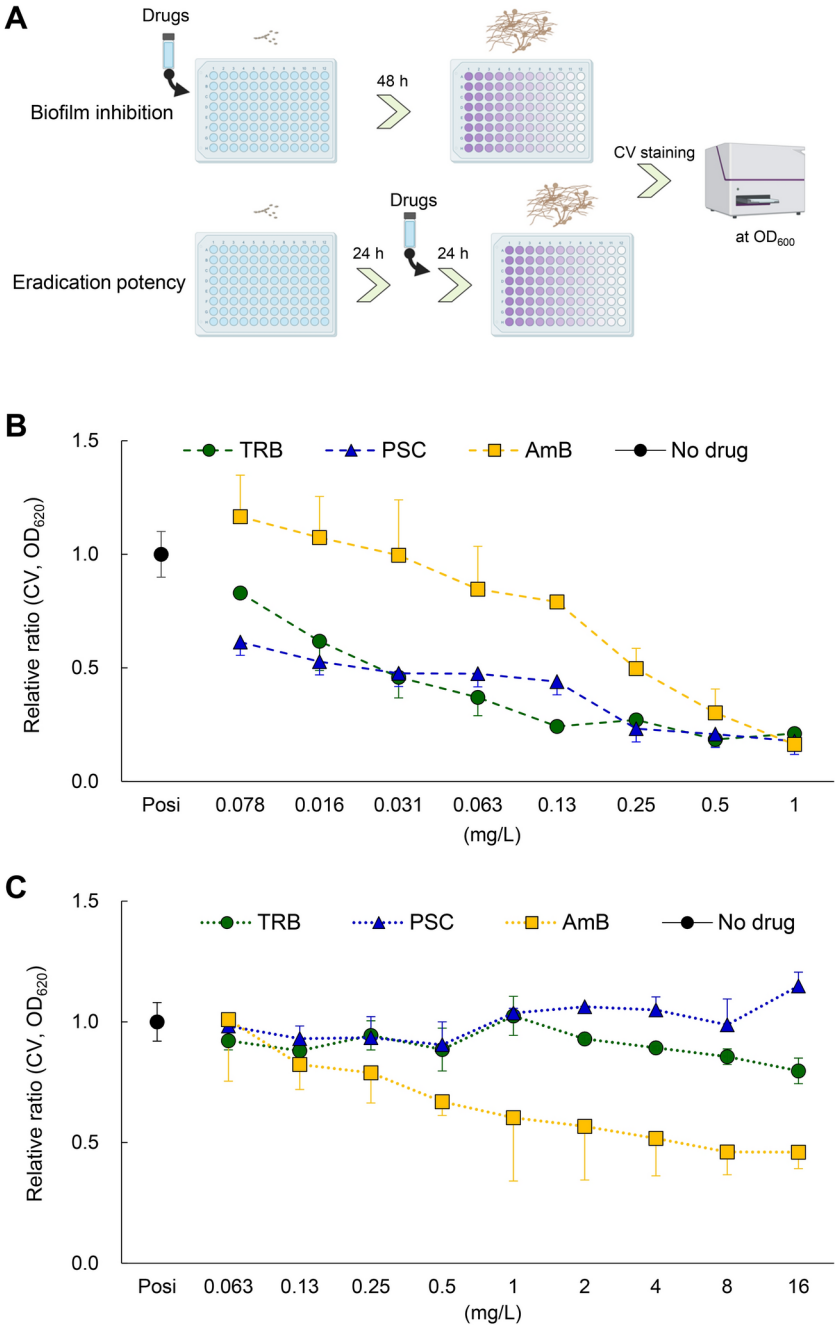

Fig. 4. Inhibition and eradication of biofilm activity of TRB, PSC, and AmB. (**A**) Schematic illustration shows assay procedures to confirm inhibition and eradication of TRB, PSC, and AmB against *E. dermatitidis* 1 biofilm. (**B**) Biofilm inhibition and (**C**) eradication potency of TRB (green circle), PSC (blue triangle), and AmB (yellow square) are shown as a relative ratio from 0.078 to 1 mg/L and from 0.063 to 16 mg/L, respectively. All assays were performed independently in triplicate. Means (±S.D.) of all data are presented.

TRB targets SQLE, a key enzyme, in ergosterol biosynthesis in fungal membranes[17,18]. The important AA residues (L393, F397, F415, and H440) of SQLE that interact with TRB have been reported in the resistance profiles of clinical isolates of *T. rubrum*[32]. We identified the AA residues of $SQLE^{ED}$ from the genome and confirmed that the AA residues at L410, F414, F432, and H459 of $SQLE^{ED}$ corresponded to those at L393, F397, F415, and H440 of $SQLE^{TR}$, respectively, indicating that there were no TRB resistance mutations against *E. dermatitidis* (Table S1 and Table S2). In the binding model, TRB formed an H-bond with Y102 and was surrounded by TRB resistance-related residues at L410, F414, F432, and H459, showing a better interaction of TRB with $SQLE^{ED}$ (Fig. 2 and Fig. S2). These data suggested that TRB can strongly bind to $SQLE^{ED}$, eliciting a potent antifungal effect.

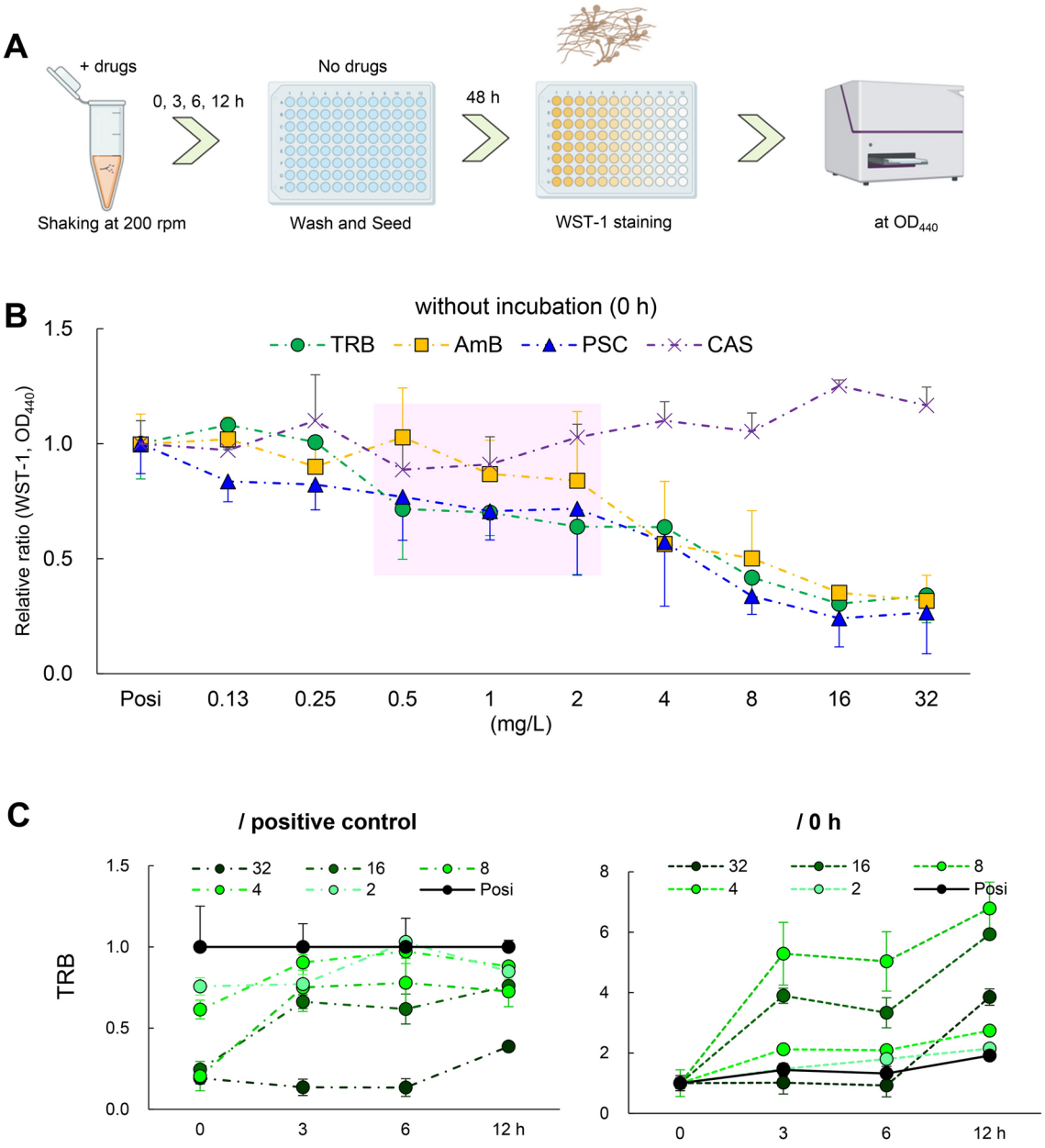

Fig. 5. PAFE and killing activity of TRB, PSC, and AmB. (**A**) Schematic illustration of assay procedures to confirm the PAFE and killing potency of TRB, PSC, and AmB against *E. dermatitidis* 1. (**B**) PAFE of TRB (green circle), PSC (blue triangle), AmB (yellow square), and CAS (purple × mark) treated with no incubation time (0 h) is shown as a relative ratio from 0.125 to 32 mg/L. Assays were performed independently in triplicate. Means (± S.D.) of all data are presented. The killing potency of (**C**) TRB, (**D**) PSC, and (**E**) AmB were evaluated and shown as relative ratios at each appropriate concentration and incubation time as assessed by cell viability using WST-1 staining. Assays were performed independently in triplicate. Means (± S.D.) of representative data are shown.

TRB shows sufficient serum concentrations[33,34] and drug transfer to the skin and nails[35], resulting in efficacy against dermatomycosis in clinical studies, but insufficient transfer to lung tissue[36,37] in animal models. Nevertheless, Oral administration of TRB has been reported to be effective in a few patients with chronic *Aspergillus* lung infections[38,39]. Clinical trials with larger numbers of patients are needed to evaluate the significant efficacy of TRB in the treatment of fungal pneumonia.

In this study, PSC, with a potent antifungal activity profile, has a different mechanism of action from that of TRB against *E. dermatitidis*. According to a report on tissue concentrations in biopsy specimens obtained at autopsy from seven patients receiving PSC prophylaxis, lung concentrations were higher than those in the plasma[40]. The formulation of PSC is mixed with hydroxy-β-cyclodextrin, which improves its antifungal activity and pharmacokinetics by enhancing its solubility and oral bioavailability[41] as well as ITC[42]. These results suggest

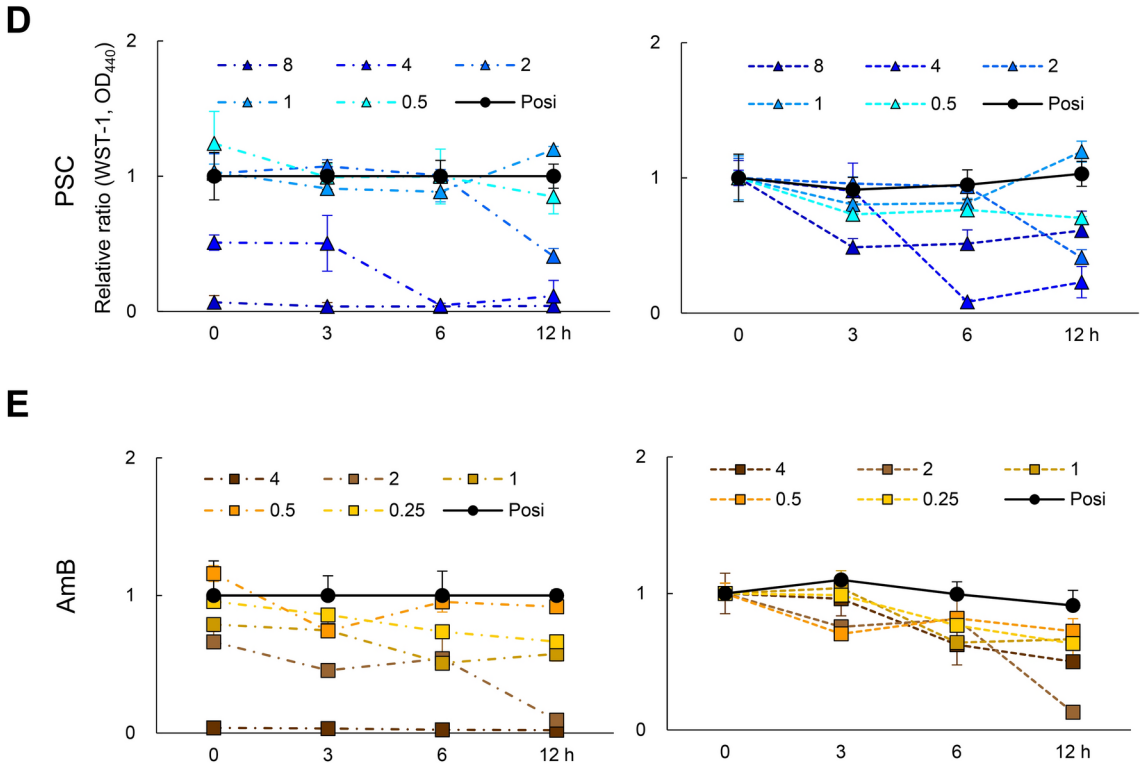

Figure 5. (continued)

that PSC with improved tissue migration may also be a suitable therapeutic option for invasive *E. dermatitidis* infections.

Recently, amikacin liposomal inhalation suspension (ALIS)[43] was developed for the treatment of refractory nontuberculous mycobacterial infectious pulmonary disease (NTM-PD) and demonstrated better efficacy in the CONVERT trial[44]. Direct administration at the site of infection, such as inhalation, can increase drug concentrations at the tissue level, resulting in greater antifungal efficacy than that of systemic administration, and leading to a reduction in the side effects of the drug. Inhalable and spray-dried microparticles of TRB[45,46] have been studied for the treatment of pulmonary fungal infections to enhance the beneficial effects of antifungal drugs as well as AmB[47]. TRB, which does not require particularly prolonged exposure (Fig. 4), would be a suitable inhaled drug for the treatment of *E. dermatitidis* pneumonia, which has been reported in approximately 6% of patients with bronchiectasis and cystic fibrosis[5]. In addition, TRB may be an additional option for therapeutic agents combined with azoles to cure invasive *E. dermatitidis* infections in immunocompromised patients[20]. We believe that re-evaluating potent old antifungals such as TRB with established efficacy and safety profiles can not only provide efficient and cost-effective treatment options for patients, leading to sustainable development goals but also help people in developing countries.

In conclusion, TRB could potentially be an even more useful and attractive antifungal drug if new routes of administration, such as inhalation or novel drug delivery systems, are developed to enhance TRB tissue migration.

Methods

Fungus and cells

E. dermatitidis 1 and 2 isolated from the patients with pneumonia were identified by ESI–MS and ITS gene analysis[15], and *E. dermatitidis* 3 (NBRC6421, ATCC28869) was purchased from Biological Resource Center, NITE (NBRC, Japan) (Table S2). The fungus was incubated in Sabouraud buffer (5 g of meat peptone, 5 g of casein peptone, and 20 g of glucose in 1L dH_2O) and Sabouraud dextrose agar (SDA) plate (5 g of meat peptone, 5 g of casein peptone, 40 g of glucose, and 1.5% agar in 1L H_2O) supplemented with chloramphenicol (Cam) and kanamycin (K), or 0.25 μm filtered RPMI (Nissui, Japan) without $NaHCO_3$ at pH 6.8, 0.165 M 3-morpholinopropane-1-sulfonic acid, MOPS (MOPS-RPMI) supplemented with Cam and K. A549 cells isolated from a male patient with lung cancer were purchased from the Japanese Collection of Research Bioresources (JCRB) Cell Bank, Japan, and cultured in DMEM medium (FUJIFILM Wako Pure Chemical Corporation, Japan) supplemented with 10% fetal bovine serum (FBS; Gibco, Thermo Fisher Scientific, USA), penicillin (P), and K.

DNA and RNA extraction, and identification of SQLE sequences

A collection of *E. dermatitidis* incubated on SDA with a small medicine spoon was completely frozen in liquid nitrogen. After grinding with a masher tube, total RNA and DNA were extracted using TRIzole (Invitrogen,

A

TRB + PSC

Drugs		TRB								
	Conc.	0.5	0.25	0.13	0.063	0.031	0.016	0.0078	0.0039	0
PSC	0.25	0.03	0.03	0.03	0.04	0.03	0.03	0.04	0.04	0.04
	0.13	0.04	0.04	0.03	0.05	0.04	0.03	0.03	0.03	0.05
	0.063	0.03	0.03	0.05	0.13*	0.37	0.17	0.24	0.21	0.72
	0.031	0.02	0.02	0.06	0.30	0.47	0.22	0.24	0.44***	0.76
	0.016	0.02	0.02	0.02**	0.34	0.49	0.63	0.58	0.61	0.84
	0	0.01	0.00	0.13	0.28	0.55	0.50	0.61	0.55	0.80

0 - 0.1 | 0.1 - 0.5 | 0.5 -

	PSC	TRB	FICI
MIC*	0.5	0.25	**0.75**
MIC_{90} WST-1**	0.5	0.13	**0.63**
MIC_{50} WST-1***	0.25	0.06	**0.31**

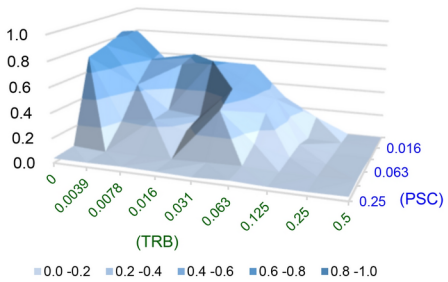

B

TRB + AmB

Drugs		TRB								
	Conc.	0.5	0.25	0.13	0.063	0.031	0.016	0.0078	0.0039	0
AmB	0.5	0.02	0.02	0.01	0.01	0.02	0.01	0.01	0.01	0.01
	0.25	0.02	0.02**	0.02	0.01	0.02	0.05	0.01	0.01	0.01
	0.13	0.02	0.02	0.12*/***	0.17	0.14	0.17	0.12	0.21	0.26
	0.063	0.03	0.03	0.39	0.75	0.68	0.52	0.78	0.50	0.76
	0.031	0.02	0.02	0.37	0.74	0.70	0.75	0.70	0.87	0.82
	0	0.01	0.01	0.23	0.57	0.70	0.89	0.95	1.02	0.87

0 - 0.1 | 0.1 - 0.5 | 0.5 -

	AmB	TRB	FICI
MIC*	0.5	0.5	**1.0**
MIC_{90} WST-1**	1.0	1.0	**2.0**
MIC_{50} WST-1***	1.0	1.0	**2.0**

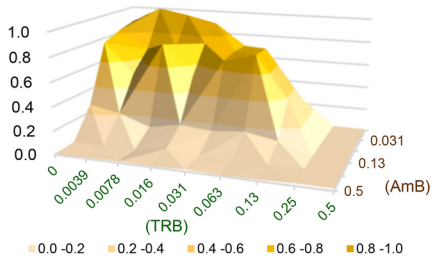

C

AmB + PSC

Drugs		AmB								
	Conc.	0.5	0.25	0.13	0.063	0.031	0.016	0.0078	0.0039	0
PSC	0.25	0.03	0.01	0.02	0.03	0.02	0.04	0.04	0.02	0.01
	0.13	0.07	0.06	0.07	0.05	0.09	0.02***	0.05	0.01	0.25
	0.063	0.02	0.03	0.06**	0.11*	0.37	0.55	0.14	0.20	0.47
	0.031	0.02	0.02	0.08	0.38	0.71	0.51	0.57	0.51	0.84
	0.016	0.03	0.03	0.09	0.34	0.90	0.73	0.69	0.60	0.93
	0	0.02	0.01	0.02	0.23	0.50	0.62	0.74	0.78	0.78

0 - 0.1 | 0.1 - 0.5 | 0.5 -

	PSC	AmB	FICI
MIC*	0.5	0.5	**1.0**
MIC_{90} WST-1**	1.0	0.5	**1.5**
MIC_{50} WST-1***	0.25	2.0	**2.25**

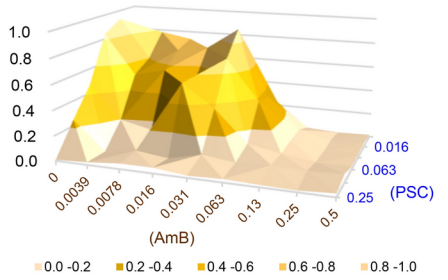

Fig. 6. Combination effect of TRB, PSC, and AmB on *E. dermatitidis*. A combination of (**A**) TRB and PSC, (**B**) TRB and AmB, and (**C**) AmB and PSC tables and 3D surface plots consist of relative ratios at each appropriate concentration as assessed by *E. dermatitidis* 1 viability using WST-1 staining. FIC indices (FICI) were evaluated as synergy; FICI < 0.5, no interaction (additive); 0.5 < FICI < 4, or antagonism; FICI > 4, which calculated from MIC (*in red) data or MIC_{50} (***) and MIC_{90} (**) of WST-1 staining results. All assays were performed independently in triplicate and representative data are shown.

	Growth Inhibition				Biofilm Inhibition		Combination
Drugs	MIC	MIC_{50}	MIC_{90}	Killing	Inhibition	Eradication	Synergy or Additive
TRB	0.25	0.13	0.25	−	+ + +	±	PSC, VRC, ITC
PSC	0.13	0.063	0.13	+ +	+ + +	−	TRB
AmB	0.13	0.063	0.13	+ + +	+	+ +	−

Table 2. Summary of versatile anti-*E. dermatitidis* activity of TRB, PSC, and AmB. MIC_{50} and MIC_{90} values were determined by measuring at OD_{530} nm. The effect of the drugs on *E. dermatitidis* 1 is shown as follows: + + +; very strong, + +; strong, +; mild, ±; weak, and −; none.

Thermo Fisher Scientific). RNA was converted into complementary DNA (cDNA) using ReverTra Ace® (TOYOBO, Japan). These primers (ITS4R: TCC TCC GCT TAT TGA TAT GC NS7F: GAG GCA ATA ACA GGT CTG TGA TGC) provided the best combination for identification with the strain of *E. dermatitidis* using the ITS sequence. PCR amplifications were performed in an Eppendorf thermocycler (Eppendorf® Mastercycler) in a final volume of 40 µL with 10–50 ng of the DNA as a template using KOD one polymerase (TOYOBO). The SQLE sequence of *E. dermatitidis* 1, 2, and 3 was identified from the cDNA using these primers (ED.SE.SF: ATG CCT CTC ATA CTC GAT TCG TCG TC, ED.SE.ER: TCA AAT CCT CAG TTC GGC AAA TAT ATA CG, ED.SE.SQF: TCT GAT TCT GGG TGT GGA GTC C, ED.SE.SQR: TCA GGT ACG TCG ACC AGG ACA CG).

SQLE 3D structure and docking simulation

The 3D structure model of $SQLE^{ED}$ was produced as a template of the crystal structure of $SQLE^{Hum}$ (PDB accession number, 6C6N) using the SWISS model (https://swissmodel.expasy.org/). A nicotinamide adenine dinucleotide (NAD) was docked to the $SQLE^{ED}$ in the same manner as the crystal structure of $SQLE^{Hum}$ using SeeSAR v13.1 software (BioSolveIT GmbH, Sankt Augustin, Germany) (https://www.biosolveit.de/products/seesar/)[48]. Subsequently, the binding pocket of TRB was identified through PDB:6C6N and clinically isolated TRB-resistant amino acid mutations of *T. rubrum*. The docking simulation of TRB to the $SQLE^{ED}$ was conducted. Molecular graphics and analyses were performed using UCSF Chimera (https://www.rbvi.ucsf.edu/chimera).

Giemsa and WST-1 staining procedures

Giemsa staining was used to observe *E. dermatitis* on A549 cells. A549 cells with or without *E. dermatitis* was washed with phosphate-buffered saline (PBS) and dried at room temperature (RT) for 30 min. They were then fixed with methanol for 5 min, stained with Giemsa dilution buffer (Merck KGaA, Darmstadt, Germany) for 20 min, washed with phosphate buffer (pH 7.2), and dried at RT for 30 min.

WST-1 staining was employed to assess the viability of *E. dermatitidis*. WST-1 staining solution was composed of 0.2 mM 1-methoxy-5-methylphenazinium methylsulfate (Dojindo, Japan), and 5 mM 2-(4-iodophenyl)-3-(4-nitrophenyl)-5-(2,4-disulfophenyl)-2H-tetrazolium, monosodium salt (Dojindo, Japan) in 20 mM HEPES buffer (pH 7.2)[21]. Before the assay, the WST-1 staining solution was stored at -80℃. A volume of 10 µL of WST-1 staining solution was added to the samples in a 96-well plate and incubated at 35℃ for 2 h in a shaking incubator. The plate absorbance was quantified at OD_{440} using an absorbance spectrometer (FLUOstar Omega, BMG Labtech, Germany).

Minimum inhibitory concentration

According to CLSI M38 3rd edition, drugs were adjusted by 1/2 dilution to the concentration tested, and *E. dermatitidis* 1, 2, and 3 were inoculated at 1.0×10^5 CFU/ml and incubated at 35℃ for 48 or 72 h in a flat-bottomed 96-well polystyrene plate with MOPS-RPMI. MIC (mg/L) represents the lowest concentration of antifungal agents that inhibited the visible growth of *E. dermatitidis*. The lowest drug concentration that inhibited 50% (MIC_{50}) or 90% (MIC_{90}) of *E. dermatitidis* growth was determined by measuring fungal growth at OD_{530} nm or fungal viability following WST-1 staining at OD_{440} nm using an absorbance spectrometer (FLUOstar Omega) in comparison with the positive control (*E. dermatitidis* without drugs in MOPS-RPMI) and the negative control (MOPS-RPMI only).

E. dermatitis morphology with or without A549 cells

The adhesion details of *E. dermatitis* on A549 cells were observed by scanning electron microscope (SEM), JSM-IT300 InTouchScope™[9,49]. A549 cells at 1.5×10^5/ml were inoculated into an 18 × 18 mm coverslip on a chamber slide II (IWAKI, Japan) filled with DMEM containing 10% FBS, P, and K. After overnight incubation in 5% CO_2 at 37℃, the final concentration of *E. dermatitis* 1 was added at 1.0×10^6 /mL to these plates, which were changed to DMEM containing 1% FBS, Cam, and K, and incubated in 5% CO_2 at 35℃. The tested drugs at 0.25 mg/L were added to the plate after 6 h. These samples were further incubated in 5% CO_2 at 35℃ for 24 or 48 h. The samples on the coverslip in the chamber slide II were fixed with 2% glutaraldehyde in 0.1 M phosphate buffer (pH 7.4) for 24 or 48 h and dehydrated through 50, 75, 90, 95, and 100% ethanol sequentially. The 100% ethanol was replaced with t-butyl alcohol to cover the samples, which were then stored at − 20℃. The frozen sample was lyophilized under a vacuum and subsequently coated with platinum for observation under SEM.

Biofilm inhibition

Biofilm inhibition was determined using the crystal violet (CV) staining assay[24]. The conidium of *E. dermatitidis* 1 was seeded at 1.0×10^5 CFU/ml in a flat-bottomed, 96-well plate with the tested drugs and incubated at 35℃ for 48 h. The antifungal activity of the tested drugs was also determined by measuring OD_{530} before CV staining. The samples were washed twice with 200 µL of PBS, and stained with 100 µL of a 0.1% CV solution for 20 min at RT. The samples were washed with 200 µL of PBS and dried at 35℃ overnight. A solution of 100 µL of 30% acetic acid was incubated for 30 min at RT to extract CV staining from the biofilm. A volume of 80 µL of the solution was transferred to a fresh 96-well plate and the samples were measured at OD_{620} nm. Biofilm inhibition by the drugs was expressed as a relative ratio compared to the positive control (*E. dermatitidis* without drugs in MOPS-RPMI) and the negative control (MOPS-RPMI only).

Biofilm eradication

A modified biofilm eradication assay was performed according to the previous report[50]. Briefly, the conidium of *E. dermatitidis* 1 was seeded at 5.0×10^5 cells/ml in a 96-well plate without the tested drugs in 100 µL of MOPS-RPMI and incubated at 35℃ for 24 h. Then, the tested drugs were added to the plate at each concentration and

further incubated at 35℃ for 24 h. The eradication ability of the tested drugs was determined by the CV staining assay described above.

The post-antifungal effects (PAFE) and time-kill assay

The PAFE and time-kill assay of *E. dermatitidis* (1.0×10^6 CFU/ml) was performed in a microtube tube with 100 µL of MOPS-RPMI medium. The PAFE of TRB, PSC, and AmB were tested at concentrations ranging from 0.13 to 32 mg/L. In the time-kill assay, a series of concentrations of TRB (ranging from 2 to 32 mg/L), PSC (from 0.5 to 8 mg/L), and AmB (from 0.25 to 4 mg/L) were prepared. The samples were shaken at 200 rpm, incubated at 35 °C for 0, 3, 6, and 12 h, respectively, and then were washed twice with 1000 µL of PBS at centrifugation of 2500 rpm for 2 min. The *E. dermatitidis* samples were duplicated (final concentration, 2.5×10^5 CFU/ml) and inoculated into a 96-well plate with 200 µL of fresh MOPS-RPMI medium without drugs at 35 °C for 48 h. The viable *E. dermatitidis* was evaluated by the WST-1 staining assay (measuring at OD_{440}). The PAFE was determined using the samples incubated for 0 h. In the time-kill assay, the relative ratios were determined by dividing the data set by the positive control (*E. dermatitidis* with dimethyl sulfoxide [DMSO] in MOPS-RPMI) or the 0-h samples *E. dermatitidis* washed after the drug treatment without incubation).

Drug combination

The drug combination assay was based on the previous report[26]. Briefly, combinations of TRB and azoles, AmB and azoles, TRB and AmB, or TRB and CAS at the tested concentration were prepared in a flat-bottomed 96-well plate with MOPS-RPMI medium. The conidium of *E. dermatitidis* was seeded at 1.0×10^5 CFU/mL and incubated at 35℃ for 48 or 72 h. MIC (mg/L) was determined by visual observation of *E. dermatitidis* growth. The MIC_{50} and MIC_{90} (mg/L) values were determined by quantifying *E. dermatitidis* viability at OD_{440} nm following WST-1 staining. The inhibition ratios of the drug combination were calculated by dividing the data set by the positive control (*E. dermatitidis* without agents in MOPS-RPMI). The FIC index (FICI) of the tested combinations was determined according to previous reports[26,51]. Synergy effect was defined as FICI < 2.0, no interaction (additive effect); 2.0 < FICI < 4.0, and antagonistic effect; FICI > 4.0 from each MIC, MIC_{50} (WST-1), and MIC_{90} (WST-1) data.

Illustration

Illustrations accompanying the experimental procedure and explanations were created using BioRender (https://www.biorender.com/): Scientific Image and Illustration Software (Simplified Science Publishing, LLC [https://www.simplifiedsciencepublishing.com/]).

Drugs

TRB, MCZ, VRC, ITC, and PSC were purchased from the Tokyo Chemical Industry Japan, FLC and AmB from Wako Japan, ISC and CAS from Selleck Chemicals USA, and MCFG from Cayman Chemical USA. These tested drugs (5–20 mM) in DMSO or appropriate solutions were stored at − 80℃. Before the assays, these drugs were prepared at appropriate concentrations in MOPS-RPMI.

Statement of experimental samples

Clinical isolate samples of organisms are not human tissue. The fungi isolated in this study were analyzed for the fungi themselves, not for events related to human health. All methods were carried out under relevant guidelines and regulations of Kumamoto University.

Data availability

Human SQLE sequences (Gene ID: 6713) and *T. rubrum* SQLE sequences (Gene ID: 10376061) were used in this study. The SQLE sequence of *E. dermatitidis* 1 identified in this study was deposited in the DNA Data Bank of Japan (DDBJ) and the NCBI GenBank database under the accession number LC829653 (https://www.ncbi.nlm.nih.gov/nuccore/LC829653). DDBJ is linked to the International Nucleotide Sequence Database, INSD. The data generated during and/or analyzed in the current study are available from the corresponding authors upon reasonable request.

Received: 24 June 2024; Accepted: 4 November 2024
Published online: 11 November 2024

References

1. Bongomin, F., Gago, S., Oladele, R. O. & Denning, D. W. Global and multi-national prevalence of fungal diseases-estimate precision. *J. Fungi* **3**, 57 (2017).
2. Brown, G. D. et al. Hidden killers: human fungal infections. *Sci. Transl. Med.* **4**, 165rv13 (2012).
3. Döğen, A. et al. Dishwashers are a major source of human opportunistic yeast-like fungi in indoor environments in Mersin, Turkey. *Med. Mycol.* **51**, 493–498 (2013).
4. Isa-Isa, R., García, C., Isa, M. & Arenas, R. Subcutaneous phaeohyphomycosis (mycotic cyst). *Clin. Dermatol.* **30**, 425–431 (2012).
5. Lebecque, P. et al. Exophiala (Wangiella) dermatitidis and cystic fibrosis prevalence and risk factors. *Med. Mycol.* **48**, S4-9 (2010).
6. Vasquez, A. et al. Management of an outbreak of *Exophiala dermatitidis* bloodstream infections at an outpatient oncology clinic. *Clin. Infect. Dis.* **66**, 959–962 (2018).
7. Kirchhoff, L., Olsowski, M., Rath, P. M. & Steinmann, J. Exophiala dermatitidis: Key issues of an opportunistic fungal pathogen. In *Virulence* 984–998 (Taylor and Francis Inc, 2019).
8. Kondori, N. et al. Analyses of black fungi by matrix-assisted laser desorption/ionization time-of-flight mass spectrometry (MALDI-TOF MS): species-level identification of clinical isolates of *Exophiala dermatitidis*. *FEMS Microbiol. Lett.* **362**, 1–6 (2015).
9. Yoshinouchi, T. et al. Diagnosis and clinical management of *Exophiala dermatitidis* pneumonia in a patient with anorexia nervosa: A case report. *Med. Mycol. Case Rep.* **42**, 100617 (2023).

10. Mpakosi, A. et al. A fatal neonatal case of fungemia due to *Exophiala dermatitidis*-case report and literature review. *BMC Pediatr.* **22**, 482 (2022).
11. Silva, W. C. et al. Species diversity, antifungal susceptibility and phenotypic and genotypic characterisation of Exophiala spp. infecting patients in different medical centres in Brazil. *Mycoses* **60**, 328–337 (2017).
12. Petranyi, G., Ryder, N. S. & Stütz, A. Allylamine derivatives: new class of synthetic antifungal agents inhibiting fungal squalene epoxidase. *Science* **224**, 1239–1241 (1984).
13. Shafiei, M., Peyton, L., Hashemzadeh, M. & Foroumadi, A. History of the development of antifungal azoles: A review on structures, SAR, and mechanism of action. *Bioorg. Chem.* **104**, 104240 (2020).
14. Brüggemann, R. J., Jensen, G. M. & Lass-Flörl, C. Liposomal amphotericin B-the past. *J. Antimicrob. Chemother.* **77**, ii3–ii10 (2022).
15. Alimu, Y., Ban, S. & Yaguchi, T. Molecular phylogenetic study of strains morphologically identified as *Exophiala dermatitidis* from clinical and environmental specimens in Japan. *Med. Mycol. J.* **63**, 1–9 (2022).
16. Naka, W., Harada, T. & Nishikawa, T. Growth temperature of pathogenic dematiaceous fungi and skin surface temperature. *Jpn. J. Med. Mycol.* **27**, 245–250 (1986).
17. Ryder, N. S. Specific inhibition of fungal sterol biosynthesis by SF 86–327, a new allylamine antimycotic agent. *Antimicrob. Agents Chemother.* **27**, 252–256 (1985).
18. Padyana, A. K. et al. Structure and inhibition mechanism of the catalytic domain of human squalene epoxidase. *Nat. Commun.* **10**, 97 (2019).
19. Ghannoum, M. A. & Rice, L. B. Antifungal agents: mode of action, mechanisms of resistance, and correlation of these mechanisms with bacterial resistance. *Clin. Microbiol. Rev.* **12**, 501–517 (1999).
20. Ramzi, S. H. T. et al. Efficacy of terbinafine and itraconazole combination therapy versus terbinafine or itraconazole monotherapy in the management of fungal diseases: A systematic review and meta-analysis. *Cureus* **15**, e48819 (2023).
21. Ishiyama, M., Miyazono, Y., Sasamoto, K., Ohkura, Y. & Ueno, K. A highly water-soluble disulfonated tetrazolium salt as a chromogenic indicator for NADH as well as cell viability. *Talanta* **4**, 1299–1305 (1994).
22. Sun, Y., Liu, W., Wan, Z., Wang, X. & Li, R. Antifungal activity of antifungal drugs, as well as drug combinations against *Exophiala dermatitidis*. *Mycopathologia* **171**, 111–117 (2011).
23. Badali, H., de Hoog, G. S., Sudhadham, M. & Meis, J. F. Microdilution in vitro antifungal susceptibility of *Exophiala dermatitidis*, a systemic opportunist. *Med. Mycol.* **49**, 819–824 (2011).
24. Sharma, S. et al. Microbial biofilm: A review on formation, infection, antibiotic resistance, control measures, and innovative treatment. *Microorganisms* **11**, 1614 (2023).
25. Kirchhoff, L. et al. Biofilm formation of the black yeast-like fungus *Exophiala dermatitidis* and its susceptibility to antiinfective agents. *Sci. Rep.* **7**, 42886 (2017).
26. Pfaller, M. A., Sheehan, D. J. & Rex, J. H. Determination of fungicidal activities against yeasts and molds: lessons learned from bactericidal testing and the need for standardization. *Clin. Microbiol. Rev.* **17**, 268–280 (2004).
27. Vitale, R. G., De Hoog, G. S. & Verweij, P. E. In vitro activity of amphotericin B, itraconazole, terbinafine and 5-fluocytosine against *Exophiala spinifera* and evaluation of post-antifungal effects. *Med. Mycol.* **41**, 301–307 (2003).
28. Hazen, K. C. Fungicidal versus fungistatic activity of terbinafine and itraconazole: an in vitro comparison. *J. Am. Acad. Dermatol.* **38**, S37-41 (1998).
29. Cuenca-Estrella, M. Combinations of antifungal agents in therapy- what value are they?. *J. Antimicrob. Chemother.* **54**, 854–869 (2004).
30. Meletiadis, J., Mouton, J. W., Meis, J. F. & Verweij, P. E. In vitro drug interaction modeling of combinations of azoles with terbinafine against clinical *Scedosporium prolificans* isolates. *Antimicrob. Agents Chemother.* **47**, 106–117 (2003).
31. Sigurgeirsson, B. et al. Long-term effectiveness of treatment with terbinafine vs itraconazole in onychomycosis: a 5-year blinded prospective follow-up study. *Arch. Dermatol.* **138**, 353–357 (2002).
32. Yamada, T. et al. Terbinafine resistance of trichophyton clinical isolates caused by specific point mutations in the squalene epoxidase gene. *Antimicrob. Agents Chemother.* **61**, e00115-e117 (2017).
33. Rojo-Solís, C. et al. Pharmacokinetics of single dose oral terbinafine in common Shelducks (*Tadorna tadorna*). *J. Vet. Pharmacol. Ther.* **44**, 510–515 (2021).
34. Leyden, J. Pharmacokinetics and pharmacology of terbinafine and itraconazole. *J. Am. Acad. Dermatol.* **38**, S42–S47 (1998).
35. Faergemann, J., Zehender, H. & Millerioux, L. Levels of terbinafine in plasma, stratum corneum, dermis-epidermis (without stratum corneum), sebum, hair and nails during and after 250 mg terbinafine orally once daily for 7 and 14 days. *Clin. Exp. Dermatol.* **19**, 121–126 (1994).
36. Bechert, U., Christensen, J. M., Poppenga, R., Fahmy, S. A. & Redig, P. Pharmacokinetics of terbinafine after single oral dose administration in red-tailed hawks (*Buteo jamaicensis*). *J. Avian Med. Surg.* **24**, 122–130 (2010).
37. Schmitt, H. J. et al. Inactivity of terbinafine in a rat model of pulmonary aspergillosis. *Eur. J. Clin. Microbiol. Infect. Dis.* **9**, 832–835 (1990).
38. Schiraldi, G. F. et al. Terbinafine versus itraconazole: a long-term, randomized, double-blind, clinical trial in chronic pulmonary aspergillosis. A pilote study. *J. Health Soc. Sci.* **1**, 47–56 (2016).
39. Schiraldi, G. F. et al. Refractory pulmonary aspergillosis: compassionate trial with terbinafine. *Br. J. Dermatol.* **134**, 25–29 (1996).
40. Blennow, O. et al. Posaconazole concentrations in human tissues after allogeneic stem cell transplantation. *Antimicrob. Agents Chemother.* **58**, 4941–4943 (2014).
41. Greer, N. D. Posaconazole (noxafil): a new triazole antifungal agent. *Bayl. Univ. Med. Cent. Proc.* **20**, 188–196 (2007).
42. Mouton, J. W. et al. Pharmacokinetics of itraconazole and hydroxyitraconazole in healthy subjects after single and multiple doses of a novel formulation. *Antimicrob. Agents Chemother.* **50**, 4096–4102 (2006).
43. Zhang, J. et al. Amikacin liposome inhalation suspension (ALIS) penetrates non-tuberculous mycobacterial biofilms and enhances amikacin uptake into macrophages. *Front. Microbiol.* **9**, 915 (2018).
44. Griffith, D. E. et al. Amikacin liposome inhalation suspension for treatment-refractory lung disease caused by Mycobacterium avium Complex (CONVERT). A prospective, open-label, randomized study. *Am. J. Respir. Crit. Care Med.* **198**, 1559–1569 (2018).
45. Almansour, K. et al. Inhalable, spray-dried terbinafine microparticles for management of pulmonary fungal infections: optimization of the excipient composition and selection of an inhalation device. *Pharmaceutics* **14**, 87 (2021).
46. Brunet, K., Martellosio, J. P., Tewes, F., Marchand, S. & Rammaert, B. Inhaled antifungal agents for treatment and prophylaxis of bronchopulmonary invasive mold infections. *Pharmaceutics* **14**, 641 (2022).
47. de Pablo, E. et al. Targeting lung macrophages for fungal and parasitic pulmonary infections with innovative amphotericin B dry powder inhalers. *Int. J. Pharm.* **635**, 122788 (2023).
48. Nakamura, T. et al. Conversion of raltegravir carrying a 1,3,4-oxadiazole ring to a hydrolysis product upon pH changes decreases its antiviral activity. *PNAS Nexus* **3**, pgad446 (2023).
49. Ichikawa, T. et al. Adherence and cytotoxicity of Candida spp. to HaCaT and A549 cells. *Med. Mycol. J.* **60**, 5–10 (2019).
50. Pierce, C. G. et al. A simple and reproducible 96-well plate-based method for the formation of fungal biofilms and its application to antifungal susceptibility testing. *Nat. Protoc.* **3**, 1494–1500 (2008).
51. Odds, F. C. Synergy, antagonism, and what the chequerboard puts between them. *J. Antimicrob. Chemother.* **52**, 1 (2003).

Acknowledgements
We thank the bacteriological examination staff of the Department of Laboratory Medicine at Kumamoto University Hospital.

Author contributions
T.N. and T.Y. designed the research and, T.N., T.Y., and M.O. performed all the experiments. T.Y., D.M., and H.N. discussed the data and supported the preparation of the research. Y.J. and Y.T. supervised the personnel and the study. T.N. and H.N. obtained the necessary funding. T.N. and T.Y. wrote the manuscript, and T.Y., D.M., Y.J., and Y.T. advised or edited the manuscript. All authors read, commented on, and approved the final manuscript.

Funding
This work was supported by the Japan Society for the Promotion of Science, KAKENHI grant number JP21K16324 (T.N.), and a grant from Kobayashi Foundation, Kobayashi pharmacy-related grant (H.N.).

Declarations

Competing interests
The authors declare no competing interests.

Additional information
Supplementary Information The online version contains supplementary material available at https://doi.org/10.1038/s41598-024-78815-3.

Correspondence and requests for materials should be addressed to T.N.

Reprints and permissions information is available at www.nature.com/reprints.

Publisher's note Springer Nature remains neutral with regard to jurisdictional claims in published maps and institutional affiliations.